Available online at www.sciencedirect.com
ScienceDirect
Journal of Catalysis 246 (2007) 10–14
JOURNAL OF CATALYSIS
www.elsevier.com/locate/jcat

Spherical polyelectrolyte brushes as carriers for platinum nanoparticles in heterogeneous hydrogenation reactions

Geeta Sharma [a], Yu Mei [a], Yan Lu [a], Matthias Ballauff [a,*], Torsten Irrgang [b], Sebastian Proch [b], Rhett Kempe [b,*]

[a] *Physikalische Chemie I, University of Bayreuth, 95440 Bayreuth, Germany*
[b] *Anorganische Chemie II, University of Bayreuth, 95440 Bayreuth, Germany*

Received 26 September 2006; revised 28 October 2006; accepted 2 November 2006

Available online 8 December 2006

Abstract

Platinum nanoparticles generated on the surface of spherical polyelectrolyte brush particles were investigated with regard to their catalytic behavior in hydrogenation reactions. No surface-active agent was needed to stabilize the platinum particles. Transmission electron microscopy demonstrated that the Pt nanoparticles are well defined with a diameter of approximately 2 nm. The catalytic activity of the immobilized Pt particles, as well as the colloidal stability of the carrier particles, were preserved over many runs. These data demonstrate that the generation and immobilization of bare metallic nanoparticles on spherical polyelectrolyte brushes generate a very robust, water-based catalyst system. Pseudo-first-order kinetics with respect to the aldehyde were observed.

Keywords: Nanoparticles; Catalysis; Spherical polyelectrolyte brush; Polyelectrolytes; Platinum; Hydrogenation

1. Introduction

Metal nanoparticles exhibit different properties than their bulk materials and their isolated atoms [1,2]. Due to quantum size effects, metal nanoparticles find applications in optics [3], microelectronics [4], surface-enhanced Raman scattering [5,6], ultrasensitive chemical sensors [7], and information storage [8]. In principle, their high surface area per volume makes metal nanoparticles ideal candidates for catalysis as well [1,9]. Catalysis by platinum nanoparticles has been the subject of numerous recent publications and has prospects for various interesting applications [10–16].

However, particles with size on the order of 2–3 nm are difficult to handle or recycle and may coagulate. Hence, practical applications of nanoparticles as catalysts require sufficient colloidal stability so that the particles do not coalesce and/or a robust carrier system suitable for the reaction under consideration. The stabilization of nanoparticles by surface layers may profoundly change their properties and may interfere with their catalytic activity. The same problem may occur when immobilizing the nanoparticles on solid substrates. Therefore, a systematic study of the catalytic behavior of inertly supported metallic nanoparticles requires a neutral robust carrier system that is easy to handle and restricts coagulation.

Recently, we presented a new method for generating metallic nanoparticles on the surface of colloidal polymer particles. This method, shown schematically in Fig. 1, uses carrier particles onto which long cationic polyelectrolyte chains are grafted. The polyelectrolyte chains are generated on the surface of the polystyrene core covered with a thin shell of photoinitiator through a "grafting from" method using photoemulsion polymerization [17]. The high grafting density leads to a strong interaction between the attached polymer chains so that the brush limit is reached. The carrier particle used herein presents cationic spherical polyelectrolyte brushes (SPBs). Anionic and cationic SPBs have been the focus of numerous recent studies [17–21]. The most important feature of these SPBs is the strong localization of the counterions, as shown schematically

* Corresponding authors.
E-mail addresses: matthias.ballauff@uni-bayreuth.de (M. Ballauff), kempe@uni-bayreuth.de (R. Kempe).

0021-9517/$ – see front matter
doi:10.1016/j.jcat.2006.11.016

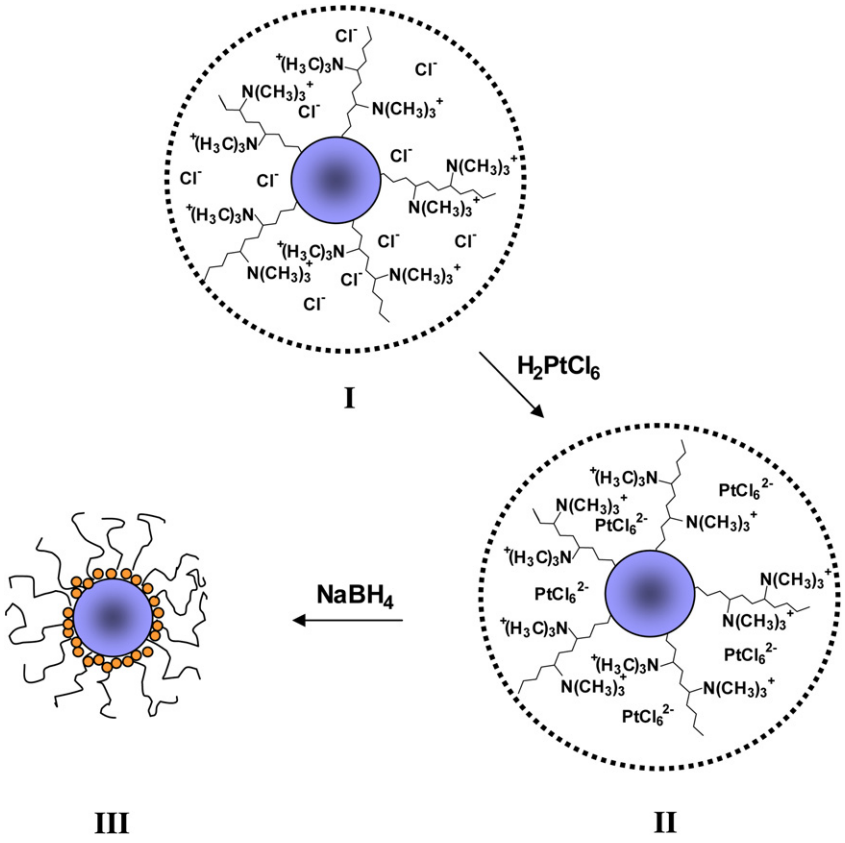

Fig. 1. Schematic representation of formation of platinum particles on the surface of the core–shell system. The core–shell system having shell of poly(2-methylpropenoyloxyethyl)trimethylammonium chloride [**I**]. **I** was counterion exchanged with $PtCl_6^{2-}$ to give **II.** $NaBH_4$ reduction of **II** forms **III** with nanosized platinum particles.

in Fig. 1. In salt-free solution, virtually all counterions are confined within the brush layer attached to the surface of the core particles. The brushes localize the counterions of the polyelectrolyte inside the structure, leaving only 2–3% of them osmotically active [19]. Hence, these counterions were reduced to yield metallic nanoparticles directly on the surface [20,21]. Moreover, it has been shown that the colloidal stability of the carrier particles bearing the nanoparticles is not impeded by this step.

In this paper we show that the spherical polyelectrolyte brushes not only lead to the formation of well-defined particles, but also act as a stable and robust carrier system. This is demonstrated by their repeated use as a catalyst in an aqueous system. Special attention is given to the stability of the catalyst after repeated use and workup.

2. Experimental

2.1. Materials

H_2PtCl_6, $NaBH_4$, and butyraldehyde (reagent grade) were received from Aldrich and used without further purification. The cationic spherical polyelectrolyte brush was synthesized and characterized as described elsewhere [20]. All pertinent parameters—namely the core radius R (46 nm), the contour length L_c (182 nm) of the attached chains, and the grafting density σ (0.019 nm^{-2}; number of polymer chains per unit area)—were determined as described previously [17].

For the synthesis of platinum nanoparticles, 3 mL of the polyelectrolyte brush system (core radii 46 nm, contour length 182 nm, solid content 15.22 wt%) was placed in an ultrafiltration cell. Ion exchange was then carried out by serum replacement against 2×10^{-3} mol/L H_2PtCl_6 solution. The white polyelectrolyte brush system turns pale yellow after the treatment with H_2PtCl_6 solution. Remaining co-ions and unbound $PtCl_6^{2-}$ ions were removed by ultrafiltration with pure water until the conductivity of the serum was reduced to 2 μs/cm. It is evident that the divalent $PtCl_6^{2-}$ ions immediately replaces the monovalent chloride ions introduced during particle synthesis. This can be inferred from the high osmotic pressure built up by the monovalent counterions fully immobilized within the brush layer. Replacing these monovalent ions by the divalent $PtCl_6^{2-}$ ions reduces the osmotic pressure within the brush layer by roughly half, followed by a marked reduction of the brush height L. Hence, stoichiometric amounts of the precious noble metal suffice for this exchange procedure.

This brush system bearing $PtCl_6^{2-}$ ions as counterions was reduced using 2×10^{-2} M solution of $NaBH_4$. Reduction with $NaBH_4$ changed the color of the latex to black. Further addition of either reagent did not produce any change in color, suggesting complete reduction of the $PtCl_6^{2-}$ ions present in the brush layer of the carrier particles. After the final addition, the latices

were stirred for another 1 h and then carefully rewashed with distilled water in an ultrafiltration cell. This process removed not only the salts from synthesis, but also a fraction of platinum particles, which was not firmly bound to the particles.

2.2. Methods

2.2.1. Catalyst synthesis and characterization

Conductometric titrations were carried out using a Q cond 2200 conductometer. Cryo-TEM specimens were prepared by vitrification of thin liquid films supported on a TEM copper grid (600 mesh, Science Services, Munich, Germany) in liquid ethane at its freezing point. The specimen was inserted into a cryotransfer holder (CT3500, Gatan, Munich, Germany) and transferred to a Zeiss EM922 EFTEM (Zeiss NTS GmbH, Oberkochen, Germany). Examinations were carried out at temperatures around 90 K. The TEM was operated at an acceleration voltage of 200 kV. Zero-loss filtered images were taken under reduced dose conditions (500–2000 e/nm^2). All images were recorded digitally by a bottom-mounted CCD camera system (Ultrascan 1000, Gatan, Munich, Germany) and processed with a digital imaging processing system (Digital Micrograph 3.9 for GMS 1.4, Gatan, Munich, Germany).

Dynamic light-scattering measurements were performed with ALV 4000 light-scattering goniometer (Peters, Germany). Most of the measurements were carried out at an angle of 90 degrees. Additional experiments carried out at different angles ensured the validity of the q^2-dependence expected for a purely diffusional motion. Moreover, a careful analysis of the correlation functions excluded the presence of aggregates or coagulation.

2.2.2. Catalytic reactions

The hydrogenation of butyraldehyde to 1-butanol was studied. The reactions were carried out in an autoclave (multiple test reactor, Paar instrument), equipped with the temperature controller 4835 (temperature range, −10 to 350 °C; pressure, up to 200 bar). The products were extracted three times with 3 mL of ether. Both the reactant and product (butyraldehyde and 1-butanol) were monitored by gas chromatography (GC). GC was carried out using an Agilent 6890N with a flame ionization detector equipped with Agilent 19091J-413, HP-5 column. For the reproducibility experiments fresh reactant was added for the next run. For the kinetic experiments, 100 μL of the sample were extracted with 1 mL of ether at regular time intervals and analyzed by GC. The optimum stirring rate was determined by increasing the stirring rate until no enhancement of the reaction rate was observed using typical catalyst concentration as used for the kinetic studies and reproducibility experiments. All experiments were carried out at 70 bar. The kinetic studies, the reproducibility studies, and especially the investigation of the dependence of the activity/conversion from the catalyst concentration are indicative that (under the optimal stirring rate and this pressure) a diffusion-controlled conversion is not very likely. To show that the catalytic activity results from the particles and not from molecular species stabilized in aqueous solution, the catalyst systems were filtered over silica multiple times. The remaining filtrates were checked for hydrogenation activity (butyraldehyde).

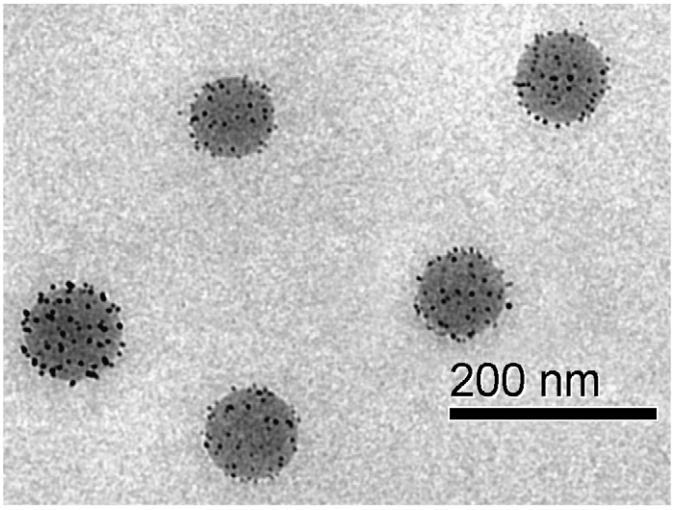

Fig. 2. Cryo-TEM image of the Pt/SPB composite nanoparticles.

3. Results and discussion

3.1. Synthesis and characterization of the composite particles

For the studies reported here, a cationic brush system with brushes of poly(2-methylpropenoyloxyethyl)trimethylammonium chloride was chosen as support. The brush polymer contains the functional group $–N(CH_3)_3^+Cl^-$, which interacts with the anions of $PtCl_6^{2-}$. The number of $–N(CH_3)_3^+Cl^-$ groups were determined by conductometric titration of the core–shell system with $AgNO_3$ solution. Accordingly, the exact amount of H_2PtCl_6 was added to the core–shell system. Once the ions are introduced into the system, they are confined due to the osmotic effect of the brush. Unbound metal ions were removed subsequently by ultrafiltration against pure water. After this step, the mixture was reduced chemically by $NaBH_4$. The color of the mixture changes from light yellow to black. The particles were stable for months.

A cryo-TEM image of the nanoparticles is shown in Fig. 2. Nearly monodisperse platinum nanoparticles with an average diameter of 2.1 ± 0.4 nm can be seen. Because the cryo-TEM was done in the frozen solvent, the exact location of the platinum nanoparticles on the carrier particles can be seen in contrast to the TEM studies in the dried state, where the drying of the Pt/SPB composite leads to collapsed brushes.

The particles are well separated from each other, because the particles have been generated by a random nucleation within the brush layer. Hence, clustering of the nanoparticles occurs only on few occasions.

3.2. Determination of active sites per particles

The number of active sites per platinum particles was determined by hydrogen adsorption studies (pulse titration) on the solid catalyst (freeze dried) at 40 °C. The freeze-dried sample

was left in high vacuum, and the mass was determined until it reached a constant value (190 mg Pt/SPB lost 10 mg of water within 2 days, i.e., 5 wt%). This sample was then used for pulse titration via a Quantachrome ChemBET 3000 TPR/TPD at room temperature. 0.165 ± 0.001 mmol of hydrogen was adsorbed per gram of the catalyst material. Considering 3.00×10^{17} platinum particles per gram of dried catalyst (estimated from TEM images), the number of hydrogen molecules adsorbed per platinum particle was found to be 478 ± 46, which has been used as an equivalent to the number of active sites.

3.3. Hydrogenation by the platinum nanoparticles

The hydrogenation of butyraldehyde to 1-butanol catalyzed by platinum nanoparticles supported on SPB particles was studied. All the reactions were carried out in aqueous solution at 40 °C and 70 bar hydrogen pressure. The reactant and product concentrations (butyraldehyde and 1-butanol) were monitored by GC.

The optimum stirring rate was determined by increasing the stirring rate until no enhancement of the reaction rate was observed. The optimum stirring rate was determined to be 300 rpm. A 2-mL catalyst solution containing 6.3×10^{15} Pt particles with a Pt surface area of (0.35 ± 0.13) m^2 or $(3.0 \pm 0.3) \times 10^{18}$ active sites was used to hydrogenate 0.11 mmol of butyraldehyde at stirring rates from 50 rpm to 400 rpm (reaction time, 1 h; pressure of H_2, 70 bar; temperature, 40 °C). The conversion to 1-butanol increased from 60% at 50 rpm to 75% at 300 rpm and maintains at this level of conversion essentially up to a stirring rate of 400 rpm. Hence, all of the experiments described below were carried out at 300 rpm to avoid diffusion-controlled runs.

The hydrogenation of the butyraldehyde also could be catalyzed by ionic or other molecular platinum species in aqueous solution. The catalyst solution was filtered over silica several times, and hydrogenation was carried out using the filtered solution. The filtrate obtained by 2 times filtration gave a conversion of <20% 1-butanol (catalyst loading, 2.5×10^{16} Pt particles; $(1.2 \pm 0.12) \times 10^{19}$ active sites; (1.4 ± 0.5) m^2 total surface area of Pt particles). The appearance of the catalyst was still hazy black, which might be due to some of the unfiltered platinum nanoparticles. Five filtrations over silica using a higher catalyst loading than for the double-filtration experiment yielded a clear filtrate that was completely inactive for hydrogenation (catalyst loading, 5×10^{16} Pt particles, $(2.4 \pm 0.24) \times 10^{19}$ active sites, (2.8 ± 1.0) m^2 total surface area of Pt particles).

The foregoing experiments indicate that the hydrogenation activity results from the nanoparticles only, because any of the ionic or molecular species in the filtrate would not have been removed by filtration and thus would have catalyzed the hydrogenation reaction after filtration. A number of catalyst systems based on nanosized particulate material were found to aggregate with increasing number of catalytic cycles, leading to reduced efficiency with every subsequent run. Hence, a study was conducted to investigate the efficiency of the catalyst after recycling. The catalyst system was used for 10 runs, with the products extracted with ether after each run. The residues of ether from the catalyst were removed by sonication at 40 °C. (The careful removal of ether is important, because any remaining ether results in decreased conversion.) An experiment carried out without sonication resulted in diminished or no activity. The conversion can be totally regained by sonication even if the run previously showed no activity. We propose the formation of hydrophobic droplets in which the educts are enriched and no interaction with the aqueous phase-based catalyst system seems possible. After complete removal of ether, fresh substrate was introduced, and the next run was carried out. A reaction time of 1 h was chosen, and the products were extracted 3 times in 3 mL of ether. Fig. 3 shows 10 runs using the same catalyst under the same reaction conditions. The efficiency of the catalyst remains unaltered during the runs. The catalyst is stable against aggregation during the runs and the workup procedure. The foregoing discussion demonstrates that the catalyst system is recyclable up to at least 10 runs without decreasing efficiency.

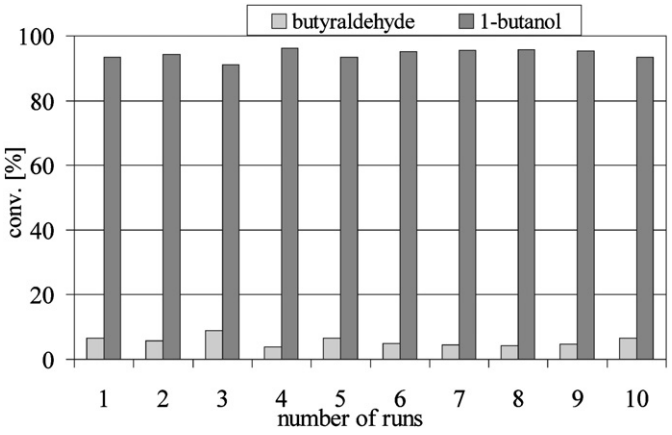

Fig. 3. Stability and re-use of the Pt/SPB composite catalyst (hydrogenation of butyraldehyde). The same catalyst was used for 10 runs. After each run products were extracted by ether (3 times with 3 mL) and fresh substrate was added. Reaction conditions: reaction time, 1 h; pressure of H_2, 70 bar; temperature, 40 °C; amount of butyraldehyde, 0.1 mL (0.11 mmol); catalyst loading, 2 mL of an aqueous solution containing 2.5×10^{16} Pt particles, $(1.2 \pm 0.12) \times 10^{19}$ active sites or (1.4 ± 0.5) m^2 total surface area of Pt particles.

The influence of the catalyst concentration on the conversion was studied to determine an optimal catalyst concentration for the kinetic experiments. For each run, the same volume of catalyst solution (2 mL) was used. The reactions were performed under 70 bar pressure of dihydrogen at 40 °C. The duration of each run was 1 h, and 0.11 mmol of substrate was used for the reactions. Products were extracted with 3 mL of ether after each run and analyzed by GC. Fig. 4 shows that the yield of butanol increased exponentially with a linear increase of the concentration of the Pt particles until 94% of conversion was reached, resulting in a TON (TON = turnover number) of 5.2 ± 0.2 per active site. The maximal conversion (94%) was observed above a catalyst loading of 2×10^{16} Pt particles or 9.6×10^{18} active sites.

Fig. 5 shows a plot of $\ln(c_{\text{butyraldehyde}}/c_{\text{butyraldehyde},0})$ vs time. A catalyst loading of 7.5×10^{15} Pt particles or $(3.6 \pm 0.36) \times 10^{18}$ active sites or (0.42 ± 0.16) m^2 total surface area of Pt particles was used. The overall kinetics of the reaction

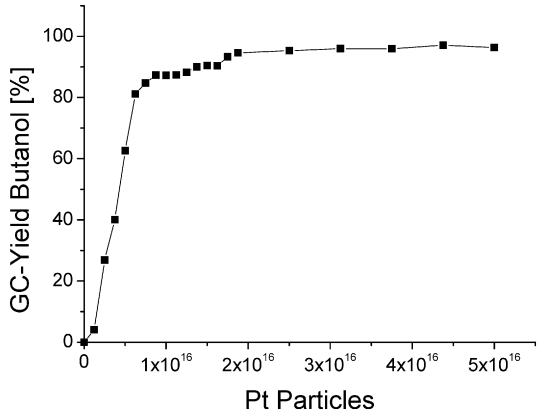

Fig. 4. The influence of catalyst concentrations on hydrogenation of butyraldehyde. Reaction conditions: time, 1 h; pressure of H_2, 70 bar; temperature, 40 °C; amount of butyraldehyde, 0.1 mL (0.11 mmol); catalyst loading, 0–5 × 10^{16} Pt particles, 0–2.4 × 10^{19} active sites.

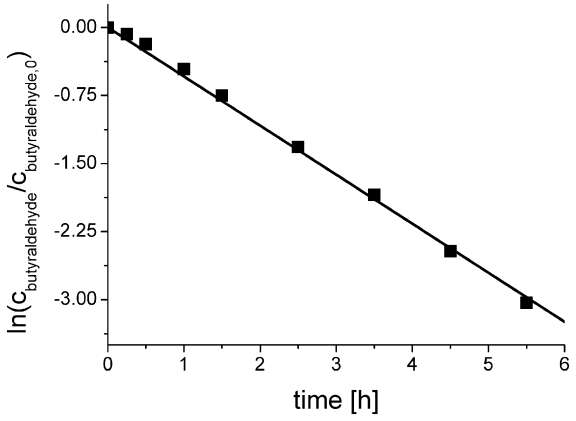

Fig. 5. Pseudo-first-order plot of the Pt/SPB composite particle catalyst system. 100 μL samples were extracted with 1 mL of ether and analyzed by GC at different times. Reaction time, 5.5 h; catalyst loading, 7.5 × 10^{15} Pt particles, (3.6 ± 0.36) × 10^{18} active sites, (0.42 ± 0.16) m^2 total surface area of Pt particles; pressure of H_2, 70 bar; temperature, 40 °C; amount of butyraldehyde, 0.2 mL (0.22 mmol).

with an excess of H_2 (70 bar) can be considered pseudo-first-order in butyraldehyde. From the slope of the linearization in Fig. 5 an apparent rate constant of $k_{\mathrm{app},70\,\mathrm{bar}} = kc_{\mathrm{H_2}}^{\beta} = (0.54 \pm 0.01)\ \mathrm{bar}^{\beta}/\mathrm{h}$ can be obtained (β = reaction order with respect to hydrogen).

It is interesting to note that our previous work showed that platinum and palladium nanoparticles prepared by the same method can be used as catalysts for the degradation of *p*-nitrophenol using $NaBH_4$ [20,21], where palladium was more effective than platinum, but their catalytic activities normalized to surface of metal particles were in the same magnitude. However, the hydrogenation activities of palladium nanoparticles were orders of magnitude smaller than those observed for the platinum system.

4. Conclusion

In conclusion, we have introduced a novel C=O hydrogenation catalyst system that works in aqueous solution under mild conditions. Product extraction was accomplished easily using a second (organic) liquid phase. An excellent recyclability concerning the catalytic performance and the product extraction was observed. The hydrogenation kinetics were best described as pseudo-first-order in butyraldehyde, and the induction period was negligible. Future work will focus on the combination with biocatalysis due to the aqueous media, on enantioselective hydrogenation, and the stabilizations of, for instance, silver- and gold-based catalysts systems as well as intermetallic nanoparticles.

Acknowledgments

Financial support by Deutsche Forschungsgemeinschaft, Sonderforschungsbereich 481, Bayreuth is gratefully acknowledged. Y. Mei and M. Ballauff thank BASF AG for financial support. This work also was supported by NanoCat, an International Graduate Program within the Elitenetzwerk Bayern. The authors thank M. Dreschler for Cryo-TEM and TEM measurements.

References

[1] L.N. Lewis, Chem. Rev. 93 (1993) 2693.
[2] A.P. Alivisatos, Science 271 (1996) 933.
[3] V.L. Colvin, M.C. Schlamp, A.P. Alivisatos, Nature 370 (1994) 354.
[4] K.D. Hermnason, S.O. Lumsdon, J.P. Williams, E.W. Kaler, O.D. Velev, Science 294 (2001) 1082.
[5] K. Svoboda, S.M. Block, Opt. Lett. 19 (1994) 930.
[6] M.J. Feldstien, C.D. Keating, Y.H. Liau, M.J. Natan, N.F. Scherer, J. Am. Chem. Soc. 119 (1997) 6638.
[7] S.R. Emory, S.J. Nie, Phys. Chem. B 102 (1998) 493.
[8] T. Sun, K. Seff, Chem. Rev. 94 (1994) 857.
[9] M. Haruta, T. Kobayashi, H. Sano, N. Yamada, Chem. Lett. (1987) 405.
[10] A.B.R. Mayer, J.E. Mark, S.H. Hausner, Angew. Makromol. Chem. 259 (1998) 45.
[11] M. Zhao, R.M. Crooks, Angew. Chem. Int. Ed. 38 (1999) 364.
[12] S.D. Jackson, G.D. McLellan, G. Webb, L. Conyers, M.B.T. Keegan, S. Mather, S. Simpson, P.B. Wells, D.A. Whan, R. Whyman, J. Catal. 162 (1996) 10.
[13] P. Concepcion, A. Corma, J. Silveatre-Albero, V. Franco, J.Y. Chane-Ching, J. Am. Chem. Soc. 126 (2004) 5523.
[14] K. Esumi, R. Isono, T. Yoshimura, Langmuir 20 (2004) 237.
[15] N. Pradhan, A. Pal, T. Pal, Colloids Surf. A 196 (2002) 247.
[16] S.K. Ghosh, M. Mandal, S. Kundu, S. Nath, T. Pal, Appl. Catal. A 268 (2004) 61.
[17] X. Guo, A. Weiss, M. Ballauff, Macromolecules 32 (1999) 6043.
[18] X. Guo, M. Ballauff, Langmuir 16 (2000) 8719.
[19] B. Das, X. Guo, M. Ballauff, Prog. Colloid Polym. Sci. 121 (2002) 34.
[20] G. Sharma, M. Ballauff, Macromol. Rapid Commun. 25 (2004) 547.
[21] Y. Mei, G. Sharma, Y. Lu, M. Ballauff, M. Drechsler, T. Irrgang, R. Kempe, Langmuir 21 (2005) 12229.